Journal of Statistical Physics, Vol. 76, Nos. 1/2, 1994

On the Brownian Motion of a Massive Sphere Suspended in a Hard-Sphere Fluid. II. Molecular Dynamics Estimates of the Friction Coefficient

Lydéric Bocquet,[1] Jean-Pierre Hansen,[1] and Jaroslaw Piasecki[1,2]

Received October 29, 1993; final March 1, 1994

The friction coefficient γ exerted by a hard-sphere fluid on an infinitely massive Brownian sphere is calculated for several size ratios Σ/σ, where Σ and σ are the diameters of the Brownian and fluid spheres, respectively. The exact microscopic expression derived in part I of this work from kinetic theory is transformed and shown to be proportional to the time integral of the autocorrelation function of the momentum transferred from the fluid to the Brownian sphere during instantaneous collisions. Three different methods are described to extract the friction coefficient from molecular dynamics simulations carried out on *finite* systems. The three independent methods lead to estimates of γ which agree within statistical errors (typically 5%). The results are compared to the predictions of Enskog theory and of the hydrodynamic Stokes law. The former breaks down as the size ratio and/or the packing fraction of the fluid increase. Somewhat surprisingly, Stokes' law is found to hold with *stick* boundary conditions, in the range $1 \leqslant \Sigma/\sigma \leqslant 4.5$ explored in the present simulations, with a hydrodynamic diameter $d = \Sigma$. The analysis of the molecular dynamics data on the basis of Stokes' law with *slip* boundary conditions is less conclusive, although the right trend is found as Σ/σ increases.

KEY WORDS: Brownian motion; hard-sphere fluid; friction coefficient; kinetic theory; Enskog theory; molecular dynamics simulations; Stokes' law.

[1] Laboratoire de Physique, École Normale Supérieure de Lyon (URA CNRS 1325), 69007 Lyon, France.

[2] Permanent address: Institute of Theoretical Physics, Warsaw University, Hoza 69, 00-681 Warsaw, Poland.

0022-4715/94/0700-0527$07.00/0 © 1994 Plenum Publishing Corporation

1. INTRODUCTION

The calculation of the friction coefficient ζ exerted by a fluid on a moving test particle is a classic problem, which was first solved, for a spherical particle, by Stokes from a macroscopic (or hydrodynamic) point of view (see, e.g., ref. 1), which applies when the suspended test particle is much larger than the molecules of the suspending fluid (or bath). However, when the size of the test particle is comparable to that of the bath molecules, a microscopic, statistical, approach becomes necessary. This has been the object of a large body of work, starting with the pioneering paper of Kirkwood,[2] who showed that the friction coefficient is given by a Green–Kubo formula, in terms of the time integral of the autocorrelation function of the instantaneous total force exerted by the bath molecules on the test particle, which we shall henceforth refer to as a Brownian particle, irrespective of its size and mass. A correct application of Kirkwood's formula poses some delicate problems associated with the order of thermodynamic and infinite-time limits, as recently reemphasized by Español and Zúñiga.[3]

In this series of papers we consider the model case where the Brownian and bath particles are elastic hard spheres. The singular nature of the "forces" during the instantaneous collisions requires a specific treatment which differs considerably from situations involving continuous dynamics. Despite these complications, the advantage of considering hard spheres is that kinetic theory for this model is in a much more advanced stage, at high densities, than for systems with continuous interactions (see, e.g., ref. 4). From a computational point of view, molecular dynamics (MD) simulations, of the type to be used in this paper, yield exact phase space trajectories, up to computer roundoff errors, for hard spheres, whereas approximate, finite-time-step algorithms have to be used to integrate the coupled equations of motion of particles interacting via continuous forces.[5]

In the first paper of this series,[6] we used an expansion in powers of the square root of the mass ratio

$$\varepsilon = \left(\frac{m}{M}\right)^{1/2} \tag{1}$$

where m and M are the bath and Brownian particle masses, to derive the Fokker–Planck equation governing the time evolution of the Brownian particle distribution, from the exact hard-sphere hierarchy of kinetic equations. The following expression was obtained for the friction coefficient $\gamma = M\zeta$ occurring in the Fokker–Planck equation:

$$\gamma = \gamma_1 + \gamma_2 \tag{2}$$

$$\gamma_1 = \left(\frac{\sigma+\Sigma}{2}\right)^2 \frac{8}{3} (2\pi m k_B T)^{1/2} \rho^{eq}\left(\frac{\sigma+\Sigma}{2}\right) \tag{3a}$$

and

$$\gamma_2 = \frac{1}{3k_B T}\int_0^\infty d\tau \, \langle \mathscr{F}_+(0)\cdot\mathscr{F}_-(-\tau)\rangle_{(\mathrm{eq}\,|\,\mathbf{X})} \tag{3b}$$

In Eq. (3a), σ and Σ are the bath and Brownian particle diameters and $\rho^{eq}((\sigma+\Sigma)/2)$ is the contact value of the equilibrium density profile of bath particles in the field of the fixed Brownian particle. The "forces" appearing in Eq. (3b) are defined by

$$\mathscr{F}_\mp = \sum_i \left(\frac{\sigma+\Sigma}{2}\right)^2 \int d\hat{\sigma}\, 2m(\mathbf{v}_i\cdot\hat{\sigma})^2\,\theta(\mp\mathbf{v}_i\cdot\hat{\sigma})\hat{\sigma} \times \delta\left(\mathbf{R} - \left(\frac{\sigma+\Sigma}{2}\right)\hat{\sigma} - \mathbf{r}_i\right) \tag{4}$$

where $\mathbf{R}$ is the (fixed) position of the Brownian particle, $\mathbf{r}_i$ and $\mathbf{v}_i$ are the position and velocity, respectively, of bath particle i at time t, θ is the Heaviside step function, and the integration is over the unit vector $\hat{\sigma}$ along the direction joining the centers of the colliding spheres. The force correlation function in Eq. (3b) involves an equilibrium statistical average of the bath in the field of the *fixed* (i.e., infinite mass) Brownian particle.

We emphasize that formulas (3) are valid for any size ratio Σ/σ, and are exact to order ε; recoil corrections, due to the finiteness of the Brownian particle mass M, only come in to order ε^2. In the small-ε limit, which we shall refer to as the Brownian limit, irrespective of the value of Σ/σ, the friction coefficient γ is thus independent of M. The first term, γ_1, is the Enskog contribution,[7] while the second, γ_2, accounts for dynamical correlations, which are not included in the Enskog approximation.

The object of the present paper is the explicit calculation of γ, for several size ratios Σ/σ and densities n of bath particles, by MD simulations. In Section 2, the expressions (2)–(4) for γ will be recast in an equivalent form, involving a force autocorrelation function, rather than the time-displaced correlation of $\mathscr{F}_+$ and $\mathscr{F}_-$; this expression will be the equivalent of Kirkwood's formula,[2] valid for continuous interactions. Three distinct routes toward explicit evaluations of γ for *finite* systems via MD simulations will be described in Sections 3–5. The first method is based on an analysis of the relaxation of the total momentum of the bath[3]; the second route proceeds from an analysis of the Laplace transform of the "force" autocorrelation function; while the third approach uses a nonequilibrium molecular dynamics (NEMD) procedure to estimate γ. Numerical results are presented in Section 6 and some final comments are contained in Section 7.

2. REFORMULATION OF THE EXACT EXPRESSION FOR THE FRICTION COEFFICIENT

The multiple-time-scale expansion in powers of ε, starting from the exact hard-sphere hierarchy of kinetic equations, led naturally in ref. 6 to the separation (2) of the friction coefficient into the Enskog term γ_1 and the dynamical correction γ_2, defined by Eqs. (3a)–(3b). A similar expansion leads, in the case of continuous interactions between particles,[8] to the Kirkwood formula:

$$\gamma = \frac{1}{3k_B T} \int_0^\infty d\tau \, \langle \mathscr{F}(0) \cdot \mathscr{F}(-\tau) \rangle_{(\text{eq} \mid \mathbf{X})} \tag{5}$$

which involves the autocorrelation function (ACF) of the total force exerted by the bath particles on the Brownian particle. It is tempting to extend formula (5) to the case of singular hard-sphere interactions, by replacing the continuous force $\mathscr{F}(t)$ by the momentum transferred from the fluid spheres to the infinitely massive Brownian sphere during instantaneous collisions, i.e.,

$$\gamma = \frac{1}{3k_B T} \int_0^\infty d\tau \, \langle \mathscr{F}_0(0) \cdot \mathscr{F}_0(-\tau) \rangle_{(\text{eq} \mid \mathbf{X})} \tag{6}$$

where

$$\mathscr{F}_0(t) = \sum_{(c)} (-2m)(\mathbf{v}_c \cdot \hat{\mathbf{r}}_c) \hat{\mathbf{r}}_c \, \delta(t - t_c) \tag{7}$$

The sum on the right-hand side (r.h.s.) of Eq. (7) is over all collisions between the immobile Brownian particle and bath particles. Each collision is an instantaneous event, taking place at time t_c, $\hat{\mathbf{r}}_c = \mathbf{r}_c / [(\Sigma + \sigma)/2]$ being the unitary vector defining the relative position of the bath particle with respect to the center of the Brownian particle at $t = t_c$, and $\mathbf{v}_c$ being the velocity of the colliding bath particle just before the collision. $\mathscr{F}_0$, as defined by Eq. (7), has the physical dimension of a force. Equations (6) and (7) have in fact been used in the molecular dynamics work of Alley and Alder,[9] who assumed the validity of this expression for the friction coefficient of a hard-sphere system by an intuitive extension of Kirkwood's relation. We are going to prove the validity of the expression (6)–(7) by showing its equivalence with the exact result derived from kinetic theory, embodied in Eqs. (2)–(3). To that purpose we first carry out the integration over angles $\hat{\sigma}$ in Eq. (4), the Brownian particle being assumed to be fixed at the origin ($\mathbf{R} = 0$), without loss of generality:

$$\mathscr{F}_{\pm}(t) = \sum_i 2m[\mathbf{v}_i(t)\cdot\mathbf{r}_i(t)]^2\,\theta(\mp\mathbf{v}_i(t)\cdot\hat{\mathbf{r}}_i(t))\,\hat{\mathbf{r}}_i(t) \times \delta\left(|\mathbf{r}_i(t)| - \frac{\sigma+\Sigma}{2}\right) \tag{8}$$

The "forces" $\mathscr{F}_{\pm}(t)$ are nonzero only at the instant of a collision between the Brownian particle and a bath particle when the distance of the center of the latter from the center of the former (i.e., from the origin) is exactly equal to $(\sigma+\Sigma)/2$. Going from the argument $|\mathbf{r}_i(t)|$ in the δ-function on the r.h.s. of Eq. (8) to the time variable, one may rewrite $\mathscr{F}_{\pm}(t)$ by summing over collisions:

$$\mathscr{F}_{\pm}(t) = \sum_{(c)} (-2m)(\mathbf{v}_c\cdot\hat{\mathbf{r}}_c)\,\hat{\mathbf{r}}_c\,\delta^{\pm}(t-t_c) \tag{9}$$

where t_c, $\hat{\mathbf{r}}_c$, and $\mathbf{v}_c$ have the same meaning as in Eq. (7). The distributions $\delta^{\pm}$ on the r.h.s. of Eq. (9) satisfy

$$\int_0^{+\infty} \delta^{\pm}(t)\,dt = \begin{cases} 1 \\ 0 \end{cases} \tag{10a}$$

$$\int_{-\infty}^{0} \delta^{\pm}(t)\,dt = \begin{cases} 0 \\ 1 \end{cases} \tag{10b}$$

The distinction between δ^+ and δ^- stems from the fact that, due to the presence of the Heaviside step function $\theta(\mp\mathbf{v}_i(t)\cdot\hat{\mathbf{r}}_i(t))$ on the r.h.s. of Eq. (8), only incoming (respectively outgoing) particles contribute to $\mathscr{F}_+$ ($\mathscr{F}_-$).

In view of the stationary property of equilibrium time-displaced correlation functions, the integral on the r.h.s. of Eq. (3b) may be rewritten, using Eq. (9), as

$$\begin{aligned}
&\int_0^{\infty} d\tau\,\langle \mathscr{F}_+(0)\cdot\mathscr{F}_-(-\tau)\rangle_{(\mathrm{eq}\,|\,\mathrm{X})} \\
&\quad = \lim_{T\to\infty}\frac{1}{T}\int_0^T dt\int_t^{\infty} ds\,\mathscr{F}_+(t)\cdot\mathscr{F}_-(s) \\
&\quad = \lim_{T\to\infty}\frac{1}{T}\int_0^T dt\int_t^{\infty} ds\left\{\sum_{(c)}\mathbf{a}_c^2\,\delta^+(t-t_c)\,\delta^-(s-t_c)\right. \\
&\qquad \left. + \sum_{(c)\neq(c')}\sum \mathbf{a}_c\cdot\mathbf{a}_{c'}\,\delta^+(t-t_c)\,\delta^-(s-t_{c'})\right\}
\end{aligned} \tag{11}$$

where the notation

$$\mathbf{a}_c = -2m(\mathbf{v}_c \cdot \hat{\mathbf{r}}_c)\,\hat{\mathbf{r}}_c \tag{12}$$

has been used. Due to the properties (10), the first term on the r.h.s. of Eq. (11) vanishes, leaving

$$\int_0^\infty d\tau\, \langle \mathscr{F}_+(0) \cdot \mathscr{F}_-(-\tau) \rangle_{(\mathrm{eq}\,|\,\mathbf{X})} = \lim_{T\to\infty} \frac{1}{T} \sum_{c=1}^{N_c(T)} \sum_{c'=c+1}^{\infty} \mathbf{a}_c \cdot \mathbf{a}_{c'} \tag{13}$$

where $N_c(T)$ is the number of collisions occurring during the time interval $[0; T]$. If ν denotes the collision rate between Brownian and bath particles, stationarity implies that the time integral (13) may be cast in the equivalent form

$$\int_0^\infty d\tau\, \langle \mathscr{F}_+(0) \cdot \mathscr{F}_-(-\tau) \rangle_{(\mathrm{eq}\,|\,\mathbf{X})} = \nu \sum_{k=1}^{\infty} \langle \mathbf{a}_c \cdot \mathbf{a}_{c+k} \rangle_c \tag{14}$$

where the statistical average is over Brownian/bath particle collisions, according to the general definition[3]

$$\langle A \rangle_c = \lim_{N_c\to\infty} \frac{1}{N_c} \sum_{c=1}^{N_c} A_c \tag{15}$$

Proceding along similar lines, one can cast the time integral of the ACF appearing in Eq. (6) in the form

$$\int_0^\infty d\tau\, \langle \mathscr{F}_0(0) \cdot \mathscr{F}_0(-\tau) \rangle_{(\mathrm{eq}\,|\,\mathbf{X})} = \nu \left\{ \frac{\langle \mathbf{a}_c^2 \rangle_c}{2} + \sum_{k=1}^{\infty} \langle \mathbf{a}_c \cdot \mathbf{a}_{c+k} \rangle_c \right\} \tag{16}$$

The first term may be explicitly calculated as[10]

$$\begin{aligned} \langle \mathbf{a}_c^2 \rangle_c &= \frac{\int d\hat{\mathbf{r}}_c \int d\mathbf{v}_c \exp\{-\beta m \mathbf{v}_c^2/2\} (\mathbf{v}_c \cdot \hat{\mathbf{r}}_c)\, \theta(\mathbf{v}_c \cdot \hat{\mathbf{r}}_c)\, \mathbf{a}_c^2}{\int d\hat{\mathbf{r}}_c \int d\mathbf{v}_c \exp\{-\beta m \mathbf{v}_c^2/2\} (\mathbf{v}_c \cdot \hat{\mathbf{r}}_c)\, \theta(\mathbf{v}_c \cdot \hat{\mathbf{r}}_c)} \\ &= 8 m k_B T \end{aligned} \tag{17}$$

Since the collision frequency ν is, for an infinite-mass Brownian particle, given by

$$\nu = 2 \left(\frac{\sigma + \Sigma}{2} \right)^2 \left(\frac{2\pi k_B T}{m} \right)^{1/2} \rho^{\mathrm{eq}} \left(\frac{\sigma + \Sigma}{2} \right) \tag{18}$$

[3] The calculational procedure and notations in this section are very similar to those used by Wainwright.[10]

it is clear from direct substitution of Eqs. (17) and (18) into Eqs. (16) and (6) that the first term on the r.h.s. of Eq. (16) yields precisely the Enskog contribution γ_1 given by Eq. (3a). Comparison of Eqs. (14) and (16) then finally shows the equivalence of expressions (2)–(3) and (6) for the friction coefficient γ. Equation (6), together with (16), is the most convenient for numerical evaluation of γ via MD simulations.

Inconsiderate application of Eq. (6) to a *finite* system, like those used in MD simulations, yields, however, $\gamma = 0$, as illustrated in Fig. 1, where the "time-dependent" friction

$$\gamma(t) = \frac{1}{3k_B T} \int_0^t d\tau \, \langle \mathscr{F}_0(0) \cdot \mathscr{F}_0(-\tau) \rangle_{(\text{eq} \mid \mathbf{X})} \tag{19}$$

is plotted versus time. This familiar pitfall has to do with an implicit inversion of limits when finite systems are being considered. As emphasized in ref. 3, a correct calculation of γ requires going first to the thermodynamic limit ($N \to \infty$, $V \to \infty$, $n = N/V$ being held fixed) for each upper integration limit t in Eq. (19), *before* taking the limit $t \to \infty$. Denoting the previously defined thermodynamic limit by limth, we find that the correct (nonzero) value of γ is given by

$$\gamma = \frac{1}{3k_B T} \lim_{t \to \infty} \int_0^t d\tau \, \text{limth} \langle \mathscr{F}_0(0) \cdot \mathscr{F}_0(-\tau) \rangle_N \tag{20}$$

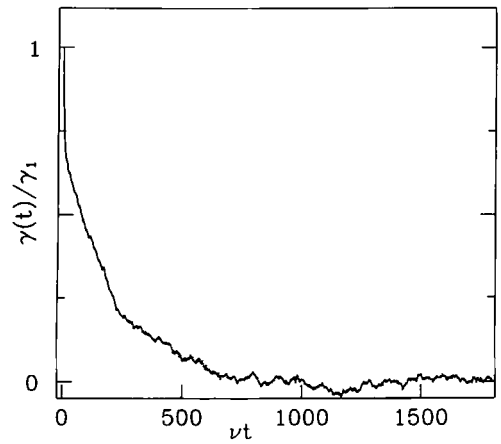

Fig. 1. Normalized "time-dependent" friction $\gamma(t)/\gamma_1$ versus reduced time νt for a system of $N = 200$ fluid particles, with an effective packing fraction $\eta_{\text{eff}} = 0.3$ (defined in Section 6), and a fixed sphere of diameter $\Sigma = \sigma$. Here $\gamma(t = 0)$ equals the Enskog value γ_1 of the friction coefficient due to the $\delta(t)$ contribution in the force ACF [see the first term in the r.h.s. of Eq. (16)].

The importance of the order of limits is illustrated by a simple model calculation in Appendix A. Three practical ways of extracing estimates of γ from MD simulations are proposed in the three subsequent sections.

In their MD simulations, Alley and Alder[9] computed $\gamma(t)$ over a shorter time interval compared to the present work; over this interval (typically $vt \sim 100$), $\gamma(t)$ does not decay to zero, and the authors used the known hydrodynamic form of the tail of the velocity autocorrelation function to extrapolate their data to infinite time; this procedure results in a nonzero value of the friction coefficient.

3. FRICTION COEFFICIENT FROM THE RELAXATION OF FLUID MOMENTUM

The first practical method which we have used to estimate γ from MD simulations is that advocated by Español and Zúñiga,[3] based on the relaxation of the total fluid momentum $\mathbf{P}(t)$. According to their analysis, which is essentially equivalent to that sketched in Appendix A, the total momentum ACF may be expected to decay exponentially [cf. Eq. (A.6)], at least for a sufficiently large test particle fixed at the origin in order for the Onsager principle to apply. Logarithmic plots of the ACF should hence yield straight lines, the negative slopes of which are directly proportional to the friction coefficient γ,

$$-\log\left[\frac{<\mathbf{P}(t)\cdot\mathbf{P}(0)>_N}{3Nmk_B T}\right]=\frac{\gamma}{Nm}\,t\equiv -\log F(t) \tag{21}$$

Examples of such plots are shown in Fig. 2. The exponential decay, implying a Markovian process, is seen to apply even for a test particle of size equal to that of the bath particles ($\Sigma=\sigma$). The observed slopes closely follow the $1/N$ size dependence. The resulting values of γ will be confronted with those obtained by the two other methods in Section 6.

4. FRICTION COEFFICIENT FROM THE LAPLACE TRANSFORM OF THE ACF

We now show that a direct numerical evaluation of the Laplace transform of the force ACF for a finite system

$$\tilde{f}_N(z)=\int_0^\infty e^{-zt}\langle \mathscr{F}_0(t)\cdot\mathscr{F}_0(0)\rangle_N\,dt \tag{22}$$

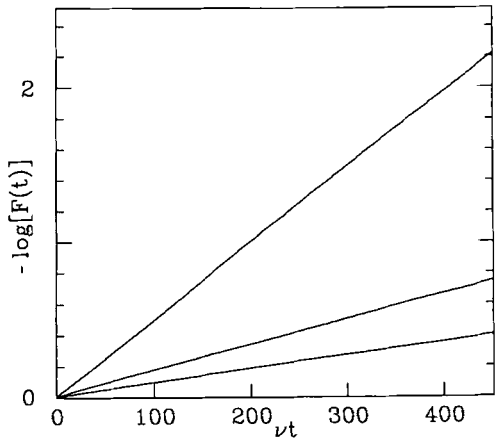

Fig. 2. Logarithmic plot of the normalized ACF, $F(t)$, of the total fluid momentum versus reduced time νt. From this plot the reduced friction coefficient $\gamma/m\nu$ is obtained as N times the slope of the straight line. The three curves were computed, from bottom to top, with systems containing $N = 800$, 500, and 200 fluid particles, with effective packing fractions $\eta_{\text{eff}} = 0.24$, 0.37, and 0.3 and a fixed sphere of diameter $\Sigma = 2.5\sigma$, 2σ, and σ, respectively.

also leads to an estimate of the friction coefficient γ. Use of Eq. (A.2) and integration by parts yields

$$\tilde{f}_N(z) = -\langle \dot{\mathbf{P}}(0) \cdot \mathbf{P}(0) \rangle_N - z \int_0^\infty e^{-zt} \langle \dot{\mathbf{P}}(t) \cdot \mathbf{P}(0) \rangle_N \, dt$$

$$= -z \int_0^\infty e^{-zt} \langle \dot{\mathbf{P}}(t) \cdot \mathbf{P}(0) \rangle_N \, dt$$

$$= \frac{3k_B T \gamma z}{z + \gamma/Nm} \tag{23}$$

where the "hydrodynamic" form (A.6) of the momentum ACF has been used; the latter is expected to apply at long times, i.e., for small values of the conjugate variable z. The left-hand side of Eq. (23) may be estimated by MD simulations. Using definition (7) of the force, one obtains

$$\tilde{f}_N(z) = \int_0^\infty e^{-zt} \langle \mathscr{F}_0(t) \cdot \mathscr{F}_0(0) \rangle_N \, dt$$

$$= \nu \left\{ \frac{\langle \mathbf{a}_c^2 \rangle_c}{2} + \sum_{k=1}^{\infty} \langle \mathbf{a}_c \cdot \mathbf{a}_{c+k} e^{-z(t_{c+k} - t_c)} \rangle_c \right\} \tag{24}$$

where the collision frequency ν is defined in Eq. (18). The quantity on the r.h.s. of Eq. (24) may be calculated by MD for several (real) values of z,

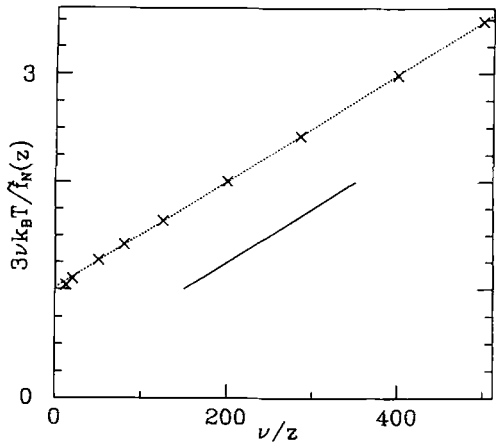

Fig. 3. Inverse of the reduced Laplace transform $3\nu k_B T/\tilde{f}_N(z)$ versus ν/z for various (real) frequencies z (crosses). The inverse of the reduced friction coefficient $\gamma/m\nu$ is obtained by extrapolating the fitted straight line to $\nu/z \to 0$ (dashed line). Its slope should be equal to $1/N$ and thus serves as a check of the simulation. The results presented were obtained for the same system as in Fig. 1. A straight line of slope 1/200 is shown for comparison with the simulation data.

and the results fitted to the r.h.s. of Eq. (23), thus yielding a direct estimate of the unknown friction coefficient γ. The procedure is illustrated in Fig. 3, where the inverse of $\tilde{f}_N(z)$ is plotted versus ν/z; the results will be discussed in Section 6. Note that taking $z=0$ leads to the interesting sum rule, valid for any finite system

$$\frac{\langle \mathbf{a}_c^2 \rangle_c}{2} + \sum_{k=1}^{\infty} \langle \mathbf{a}_c \cdot \mathbf{a}_{c+k} \rangle_c = 0 \tag{25}$$

The present derivation of γ assumes the validity of the form (A.6) for the momentum ACF, which we have explicitly checked by MD simulations as shown in Section 3 and Fig. 2. In Appendix B, we present an alternative method for extracting γ from the Laplace transform $\tilde{f}_N(z)$, without explicitly assuming the exponential form of the momentum ACF. For small enough values of z the method of Appendix B is equivalent to the one sketched in this section.

5. NEMD ESTIMATE OF THE FRICTION COEFFICIENT

Linear transport coefficients may be calculated either by Green–Kubo formulas like Eq. (6), based on the relaxation of spontaneous thermal fluctuations of the system at equilibrium, or by measuring the response of the system to a weak external perturbation, as simulated by nonequilibrium

molecular dynamics (NEMD).[11,12] In order to determine γ by NEMD, we consider the following process. Starting from an initial equilibrium situation, the infinite-mass test particle is set in motion at $t=0$ and pulled through the fluid at a constant velocity $\mathbf{u}$. The fluid, which was initially at rest, will, after a transient regime, relax toward a stationary state. This relaxation may be characterized by the time dependence of the fluid (or center-of-mass) velocity:

$$\mathbf{v}(t)=\frac{1}{Nm}\langle \mathbf{P}(t)\rangle_N \tag{26}$$

and of the temperature, which increases due to dissipation. The drift velocity $\mathbf{u}$ of the test particle will be chosen sufficiently small, so that the hard-sphere bath may be assumed to be capable of relaxing all stresses and inhomogeneities instantaneously (adiabatic assumption); in particular, the bath temperature may be regarded as homogeneous.

Under these conditions, the relaxation of the fluid velocity and of its internal energy $\mathscr{U}$ are governed by the coupled phenomenological equations

$$\frac{d\mathbf{v}(t)}{dt}=-\gamma[\mathbf{v}(t)-\mathbf{u}] \tag{27}$$

$$\frac{d\mathscr{U}(t)}{dt}=\gamma[\mathbf{v}(t)-\mathbf{u}]^2 \tag{28}$$

The second equation is an expression of the first principle of thermodynamics (the increase of $\mathscr{U}$ is equal to the rate of frictional dissipation). Since for hard spheres the internal energy reduces to the thermal kinetic energy of the particles, Eq. (28) determines the time dependence of the temperature

$$\frac{3}{2}Nmk_B\frac{dT(t)}{dt}=\gamma[\mathbf{v}(t)-\mathbf{u}]^2 \tag{29}$$

Moreover, the temperature dependence of the friction coefficient is trivial for hard spheres, since a simple scaling argument shows that it is proportional to the collision frequency ν, which, according to Eq. (18), varies as $\sqrt{T}$. Hence, choosing the initial temperature T_0 of the fluid as a reference temperature, for which $\gamma=\gamma_0$, we may write $\gamma=\gamma_0(T/T_0)^{1/2}$ and hence the system of coupled equations to be solved reads

$$\frac{d\mathbf{v}(t)}{dt}=-\gamma_0\left(\frac{T(t)}{T_0}\right)^{1/2}[\mathbf{v}(t)-\mathbf{u}] \tag{30}$$

$$\frac{3}{2}Nmk_B\frac{dT(t)}{dt}=\gamma_0\left(\frac{T(t)}{T_0}\right)^{1/2}[v(t)-u]^2 \tag{31}$$

where $v(t)=|\mathbf{v}|$ [note that $\mathbf{v}(t)$ can only be parallel to $\mathbf{u}$].

The system (30)–(31) is easily solved as shown in Appendix C. The solution is

$$\frac{T(t)}{T_f} = \left\{ \frac{(T_0/T_f)^{1/2} + \tanh[(\gamma_0/mN)(T_f/T_0)^{1/2}\, t]}{1 + (T_0/T_f)^{1/2} \tanh[(\gamma_0/mN)(T_f/T_0)^{1/2}\, t]} \right\}^2 \tag{32}$$

$$v(t) = u\left[1 - \left(\frac{T_f - T(t)}{T_f - T_0}\right)^{1/2}\right] \tag{33}$$

where $T_f = T_0 + \frac{1}{3}mu^2$ denotes the final temperature of the fluid (stationary state).

In the NEMD simulations, $T(t)$ is calculated from

$$\frac{3}{2}Nk_B T(t) = \frac{m}{2}\sum_{i=1}^{N}[v_i^2 - v^2(t)] \tag{34}$$

and $v(t)$ is obtained by averaging the fluid velocity over n independent cycles of the above-mentioned nonequilibrium procedure. The value of γ_0 may then be extracted by fitting the measured relaxation of the temperature to the theoretical prediction (32). An example is shown in Fig. 4, illustrating the excellent agreement between the equilibrium MD and NEMD estimates of the friction coefficient.

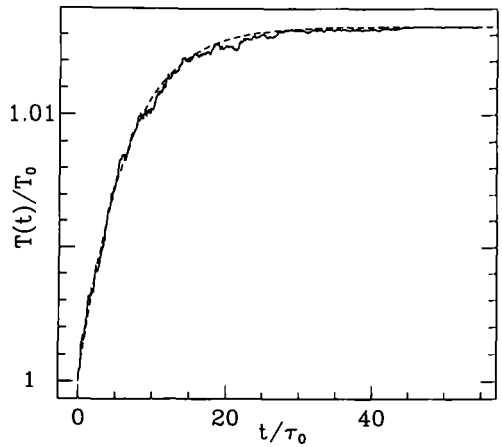

Fig. 4. Evolution of the normalized temperature $T(t)/T_0$ of the fluid as a function of reduced time t/τ_0 [$\tau_0 = (m\sigma^2/k_B T)^{1/2}$] when the infinitely massive sphere is pulled at a constant velocity u. The solid line is obtained by averaging over 50 cycles in a NEMD simulation of a system characterized by $N = 200$, $\eta_{eff} = 0.35$, $\Sigma/\sigma = 1.5$, and $u = 0.2\sigma/\tau_0$. The dashed line is the solution of the phenomenological equations (27)–(28) with $\gamma/m\tau_0^{-1} = 16.28$.

6. NUMERICAL RESULTS

The three aforementioned methods have been used to compute the friction coefficient γ for various size ratios Σ/σ and densities of the suspending fluid. It is convenient to define the effective packing fraction of the latter from the number N of spheres and the volume V' accessible to their centers in the simulation cell of total volume V, namely $V' = V - (\pi/6)(\Sigma + \sigma)^3$, according to

$$\eta_{\text{eff}} = \frac{\pi}{6}\frac{N}{V'}\sigma^3 \tag{35}$$

A summary of all runs carried out in the present study is given in Table I. The number N of spheres in the simulation cell was increased, for increasing ratios Σ/σ, in order to ensure that the box length $L = V^{1/3}$ was always significantly larger than the diameter Σ of the fixed sphere ($L \gtrsim 4\Sigma$ throughout), in order to avoid unwanted interference effects between the velocity fields around periodic images. The results reported by Alley and

Table I. List of MD Runs[a]

N	Σ/σ	η_{eff}	ν^*	γ^*	$\Delta(\gamma^*)$	γ/γ_1
108	1.0	0.15	2.16	1.12	0.04	0.84
108	1.0	0.24682	4.86	1.02	0.02	0.76
200	1.0	0.24682	4.83	1.01	0.04	0.75
200	1.0	0.3	7.02	1.01	0.03	0.75
200	1.0	0.35	10.10	0.95	0.03	0.71
500	1.0	0.35	9.98	0.90	0.04	0.67
200	1.5	0.35	18.09	0.90	0.04	0.67
500	2.0	0.24682	12.32	0.82	0.04	0.61
500	2.0	0.3	18.46	0.72	0.05	0.54
500	2.0	0.35	26.84	0.72	0.03	0.54
500	2.0	0.37	31.07	0.76	0.04	0.57
800	2.5	0.24682	17.52	0.68	0.04	0.51
800	3.0	0.24682	23.39	0.63	0.03	0.47
1500	4.0	0.24682	38.04	0.53	0.03	0.39
1800	4.5	0.24682	46.66	0.49	0.04	0.36

[a] The first three columns give, respectively, the number of fluid particles, the ratio of Brownian to fluid particle diameters, and the effective packing fraction of the bath. The last four columns list the different quantities computed in the simulations. Column 4 gives the dimensionless collision frequency $\nu^* = \nu(m\sigma^2/k_B T)^{1/2}$ between the fluid and the fixed Brownian particle; column 5 is the value of the dimensionless friction coefficient $\gamma^* = \gamma/m\nu$; the estimated error of this value is given in column 6; and column 7 gives the ratio between the computed friction coefficient γ and its Enskog value γ_1 as defined in Eq. (3a).

Alder[9] are generally for larger system sizes, but those corresponding to comparable physical conditions are compatible with the present results. The dimensionless rate of collisions between the fixed Σ-sphere and the σ-spheres, $\nu^* = \nu(m\sigma^2/k_B T)^{1/2}$, was estimated by direct counting during the MD runs. The measured values, listed in Table I, are in good agreement with the collision frequencies estimated from Eq. (18) on the basis of the scaled particle approximation[13] for $\rho^{eq}((\sigma+\Sigma)/2)$; the latter estimates lie typically 2–3% above the MD data, because scaled particle theory slightly overestimates the contact value of ρ^{eq}. All runs extended over 20×10^6 collisions, of which at least 10^5 were collisions suffered by the fixed Σ-sphere.

The values of reduced friction coefficient $\gamma^* = \gamma/m\nu$ listed in Table I are averages of the estimates based on the three independent methods of calculation sketched in Sections 3–5, respectively. The largest deviation of these estimates from the mean $\Delta(\gamma^*)$ is also given for each run; this crude estimate of the error bar suggests a statistical uncertainty of typically 5% on γ.

According to Eqs. (3a) and (18), the Enskog value of the reduced friction coefficient is just

$$\gamma_1^* = \frac{\gamma_1}{m\nu} = \frac{4}{3} \tag{36}$$

The ratio of the "exact" (MD) and Enskog values of the friction coefficient is also shown in Table I. The ratio γ/γ_1 is always less than one and, as expected, the agreement between γ and γ_1 worsens as the packing fraction η_{eff} increases, for fixed size ratio Σ/σ, or as Σ/σ increases, for fixed η_{eff}.

It is also of interest to correlate the calculated values of γ with estimates based on the familiar Stokes relation derived from macroscopic hydrodynamics,[1] namely, with stick boundary conditions,

$$\gamma_S = 3\pi\eta d \tag{37}$$

or with slip boundary conditions,

$$\gamma_S = 2\pi\eta d \tag{38}$$

where η is the shear viscosity of the suspending fluid, calculated for a packing fraction η_{eff}, and d is a suitably chosen hydrodynamic diameter. It is clear that, in view of the size ratios investigated here, the comparison with the predictions of a hydrodynamic calculation are of a purely indicative and phenomenological nature. In particular, a fully meaningful comparison should be made with the results of a hydrodynamic calculation under identical periodic boundary conditions. We did not attempt such a nontrivial

calculation, and believe that it would be more instructive to investigate larger system sizes in order to reduce the influence of the periodic boundaries and to explore any systematic N dependence.

If stick boundary conditions are assumed [Eq. (37)], the optimum hydrodynamic diameter is found to be very close to the bare diameter Σ and nearly independent of the size ratio Σ/σ. This is illustrated in Fig. 5a, where the ratio $\gamma/(3\pi\eta\Sigma)$ (with η taken from the work of Alder *et al.*[14]) is

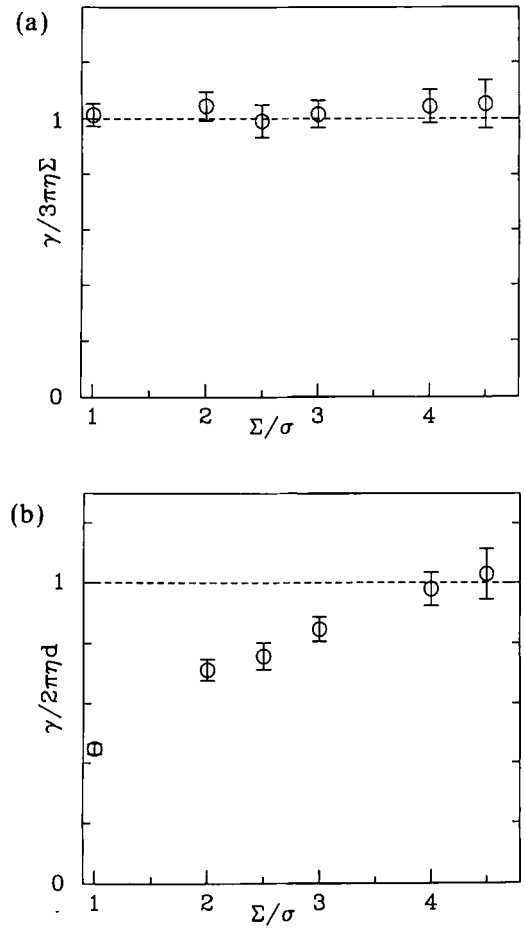

Fig. 5. (a) Ratio of the friction coefficient γ over its "stick" Stokes' value $3\pi\eta d$ as a function of size ratio Σ/σ for $\eta_{\text{eff}}=0.24682$. The "hydrodynamic" diameter of the Brownian sphere is taken to be $d=\Sigma$. (b) Same as above, but assuming slip boundary conditions with $d=\Sigma+2.4\sigma$ (see text).

plotted versus the size ratio Σ/σ. The apparent validity of stick boundary conditions is rather unexpected, and may be an artifact of applying a macroscopic relation to the case of modest size ratios.

Rather, we expect slip boundary conditions to hold in the limit $\Sigma \gg \sigma$, where d should coincide with Σ. When the ratio Σ/σ is finite (but still much larger than 1), the hydrodynamic diameter d may be somewhat larger than Σ, with the slip boundary condition applied at a certain distance from the surface of the Brownian sphere. In the case of plane walls, it has been shown that the hydrodynamic boundary condition on the velocity field applies at a surface that is separated from the solid by about one layer of fluid atoms.[15] If we assume this result to be still valid in the vicinity of a curved surface, we should identify the hydrodynamic radius of the Brownian sphere with the first minimum in $\rho^{eq}(r)$, which occurs at about $\frac{1}{2}\Sigma + 1.2\sigma$, so that the appropriate hydrodynamic diameter d should be roughly equal to $\Sigma + 2.4\sigma$; this effective diameter may vary with the packing fraction of the suspending fluid. In Fig. 5b, the resulting ratio $\gamma/(2\pi\eta d)$ is plotted versus Σ/σ. As expected, the ratio is seen to approach 1 for large size ratios, but simulations for still larger size ratios are clearly needed to confirm this trend.

7. CONCLUSIONS

In this paper we have presented numerical estimates of the friction coefficient exerted by a fluid on a moving test particle in the model case where the Brownian and solvent particles are elastic hard spheres. Three independent methods have been devised and used to compute the value of the friction coefficient from simulations of a finite system. In the first two methods use was made of the natural link between the thermal fluctuations of the fluid in the presence of the (immobile) sphere and the phenomenological friction coefficient γ. The third approach is different in spirit since it considers γ as the susceptibility of the system under the action of a weak external perturbation. All three methods lead to comparable values of the friction coefficient within an accuracy of 5%.

As expected, the Enskog approximation for the friction coefficient breaks down as the packing fraction η_{eff} and/or the size ratio Σ/σ increase. This is due to the increasing importance of dynamical correlations in the fluid arising from recollision events between the suspending fluid and the Brownian particle.

For a fixed packing fraction we compared the computed friction coefficient with its stick or slip Stokes estimate, involving the "hydrodynamic diameter" d of the Brownian particle. Somewhat surprisingly, the assumption of the stick boundary condition leads to a hydrodynamic diameter d

which is nearly independent of the size ratio Σ/σ and close to Σ. Nevertheless, in the macroscopic regime ($\Sigma \gg \sigma$) we rather expect the slip assumption to hold, with a hydrodynamic diameter d which should not differ significantly from Σ. For lower size ratios d should still be somewhat larger than Σ, since the slip boundary condition (inherent in the hydrodynamic calculation) is expected to apply at a distance slightly inside the fluid (approximately the thickness of one layer of fluid atoms). The ratio between the computed friction coefficient and its Stokes value seems to tend toward 1, which would validate the previous estimate of the hydrodynamic diameter for large size ratios. However, a definitive validation of this result requires larger-scale simulations for significantly larger size ratios than those explored here ($\Sigma/\sigma \leqslant 4.5$). The present results suggest that a crossover from stick to slip boundary condition may take place at some intermediate size ratio Σ/σ.

APPENDIX A. THE ORDER OF LIMITS IN THE CALCULATION OF THE FICTION COEFFICIENT

Consider a finite, periodic system of N spheres of mass m enclosed in a volume V in the presence of an infinitely massive test particle (the Brownian particle) fixed at the origin. Let

$$\mathbf{P}(t) = \sum_{i=1}^{N} m\mathbf{v}_i(t) \equiv Nm\mathbf{v}(t) \tag{A.1}$$

denote the total momentum of the N spheres (the bath) and $\mathbf{v}(t)$ the center-of-mass (or fluid) velocity; $\mathbf{P}$ and $\mathbf{v}$ fluctuate because of collisions with the test particle. Since $\mathscr{F}_0(t)$, defined in Eq. (6), is the instantaneous rate of momentum transferred from the bath to the test particle, we must have

$$\mathscr{F}_0(t) = -\dot{\mathbf{P}}(t) \tag{A.2}$$

where the dot denotes a time derivative. Hence

$$\lim_{t\to\infty} \int_0^t \operatorname{limth} \langle \mathscr{F}_0(0) \cdot \mathscr{F}_0(-\tau) \rangle_N \, d\tau = -\lim_{t\to\infty} \operatorname{limth} \langle \dot{\mathbf{P}}(t) \cdot \mathbf{P}(0) \rangle_N \tag{A.3}$$

Now consider a thermal fluctuation of the momentum of the bath. If the Brownian particle is sufficiently large, the regression of the fluctuation must be, according to Onsager's principle, governed by the macroscopic equations of hydrodynamics. According to the latter, the force exerted by the

flowing fluid on the Brownian particle is proportional to the momentum $\mathbf{P}(t)$ carried by the fluid, i.e., to the fluid velocity $\mathbf{v}(t) = \mathbf{P}(t)/Nm$,

$$\mathscr{F}_0(t) = \gamma \mathbf{v}(t) = \frac{\gamma}{Nm} \mathbf{P}(t) \tag{A.4}$$

or equivalently, in view of (A.2)

$$\dot{\mathbf{P}}(t) = -\frac{1}{\tau_N} \mathbf{P}(t) \tag{A.5}$$

where the momentum relaxation time is $\tau_N = Nm/\gamma$. Hence

$$\begin{aligned} <\mathbf{P}(t) \cdot \mathbf{P}(0)>_N &= \langle |\mathbf{P}|^2 \rangle_N e^{-t/\tau_N} \\ &= 3Nmk_B T e^{-t/\tau_N} \end{aligned} \tag{A.6}$$

It follows that

$$\begin{aligned} -<\dot{\mathbf{P}}(t) \cdot \mathbf{P}(0)>_N &= \frac{3Nmk_B T}{\tau_N} e^{-t/\tau_N} \\ &= 3k_B T \gamma e^{-t/\tau_N} \end{aligned} \tag{A.7}$$

When applied to (A.7), the order of limits in Eq. (A.3) yields the friction coefficient

$$-\lim_{t \to \infty} \operatorname{limth} <\dot{\mathbf{P}}(t) \cdot \mathbf{P}(0)>_N = 3k_B T \gamma \tag{A.8}$$

while inversion of the limits always leads to a vanishing result:

$$-\operatorname{limth} \lim_{t \to \infty} <\dot{\mathbf{P}}(t) \cdot \mathbf{P}(0)>_N = 0 \tag{A.9}$$

APPENDIX B. SMALL-Z LIMIT OF THE LAPLACE TRANSFORM OF THE FORCE ACF

A standard generalized Langevin (or memory function) analysis (see, e.g., ref. 16) of the time evolution of the total momentum ACF leads to the following relation between the Laplace transforms $\tilde{f}_N(z)$ and $\tilde{f}_N^{\dagger}(z)$ of the force $\mathscr{F}_0(t)$ [cf. Eq. (7)] and of the projected force $\mathscr{F}_0^{\dagger}(t)$, i.e., the component of $\mathscr{F}_0(t)$ orthogonal to $\mathbf{P}$,[3]

$$\tilde{f}_N^{\dagger}(z) = \frac{\tilde{f}_N(z)}{1 - \tilde{f}_N(z)/[(3Nmk_B T)z]} \tag{B.1}$$

Taking the thermodynamic limit of both sides of this relation, we find, remembering Eqs. (20) and (22), that

$$\gamma^{\dagger} \equiv \frac{1}{3k_B T}[\lim_{\mathrm{th}} \tilde{f}_N^{\dagger}(z)]_{z=0} = \gamma \tag{B.2}$$

However, while for a finite system $\tilde{f}_N(z=0)=0$, this is no longer true of $\tilde{f}_N^{\dagger}(z)$, which has a finite value in the limit $z \to 0$ for any N. Hence in view of Eq. (B.1), we may expect the nonzero thermodynamic limit

$$\gamma = \frac{1}{3k_B T}[\lim_{\mathrm{th}} \tilde{f}_N(z)]_{z=0} \tag{B.3}$$

to differ from $\gamma_N^{\dagger} = \tilde{f}_N^{\dagger}(z=0)/3k_B T$ only by a $1/N$ correction. $\tilde{f}_N^{\dagger}(z=0)$ may be estimated by substituting the small-z expansion of $\tilde{f}_N(z)$ into the r.h.s. of Eq. (B.1). Due to the fact that the Brownian test particle is fixed (infinite mass), the force ACF should not exhibit a long-time tail associated with hydrodynamic backflow effects,[17] so that $\tilde{f}_N(z)$ may be assumed to be analytic in the $z \to 0$ limit:

$$\tilde{f}_N(z) = az + bz^2 + \mathcal{O}(z^3) \tag{B.4}$$

and hence

$$\tilde{f}_N^{\dagger}(z) = \frac{az + bz^2 + \mathcal{O}(z^3)}{1 - a/3Nmk_B T - (b/3Nmk_B T)z + \mathcal{O}(z^2)} \tag{B.5}$$

Since $\tilde{f}_N^{\dagger}(z=0) \neq 0$, we necessarily have

$$a = 3Nmk_B T \tag{B.6}$$

and we are left with

$$\gamma_N^{\dagger} = \frac{1}{3k_B T}\tilde{f}_N^{\dagger}(z=0) = -\frac{3N^2 m^2 k_B T}{b} \tag{B.7}$$

The coefficients a and b follow from a formal expansion of the r.h.s. of Eq. (24) in powers of z, i.e.,

$$a = -\sum_{k=1}^{\infty} \langle \mathbf{a}_c \cdot \mathbf{a}_{c+k}[v(t_{c+k} - t_c)] \rangle_c \tag{B.8}$$

and

$$b = \frac{1}{2v}\sum_{k=1}^{\infty} \langle \mathbf{a}_c \cdot \mathbf{a}_{c+k}[v(t_{c+k} - t_c)]^2 \rangle_c \tag{B.9}$$

In principle, the right-hand sides of Eqs. (B.8) and (B.9) may be estimated from MD simulations; since a is known exactly from Eq. (B.6), the calculation of (B.8) could serve as a check of the simulation, while the calculation of (B.9) would yield an estimate of $\gamma_N^{\dagger}$ via Eq. (B.7), and hence of γ, within a correction $\mathcal{O}(1/N)$. This procedure for obtaining γ was not attempted here, because the quantity to be averaged in Eq. (B.9) may be expected to exhibit large statistical fluctuations due to the rapidly increasing factor $(t_{c+k}-t_c)^2$ which gives considerable weight to the correlation $\mathbf{a}_c \cdot \mathbf{a}_{c+k}$ of collisions widely separated in time.

The important point, however, is that the coefficients a and b of the Taylor expansion of $\tilde{f}_N(z)$ as given by Eqs. (B.6) and (B.7) agree with those obtained by expanding the r.h.s. of Eq. (23), based on the (reasonable) assumption of exponential decay of the momentum ACF [cf. Eq. (A.6)]. The procedure for obtaining γ described in Section 4 is thus seen to have more general validity.

APPENDIX C. VARIATION OF TEMPERATURE WITH TIME IN NEMD SIMULATIONS

The resolution of the system of differential equations (30)–(31) is simplified by using dimensionless variables defined by

$$x=\frac{v-u}{(k_B T_0/m)^{1/2}}; \qquad y=\frac{T}{T_0}; \qquad \tau=\frac{\gamma_0}{Nm}t \tag{C.1}$$

The system to be solved then reads

$$\frac{dx}{d\tau}=-\sqrt{y}\,x \tag{C.2}$$

$$\frac{dy}{d\tau}=\frac{2}{3}\sqrt{y}\,x^2 \tag{C.3}$$

supplemented by the initial conditions

$$\begin{aligned} x(\tau=0)&=\frac{-u}{(k_B T_0/m)^{1/2}} \\ y(\tau=0)&=1 \end{aligned} \tag{C.4}$$

Multiplying both sides of (C.2) by x and inserting into (C.3), one finds

$$\frac{dy}{d\tau}=\frac{2}{3}\frac{d\frac{1}{2}x^2}{d\tau} \tag{C.5}$$

so that, with the use of (C.4),

$$y(\tau) - 1 = -\tfrac{1}{3}[x^2(\tau) - x^2(0)] \tag{C.6}$$

We thus obtain a closed equation for y:

$$\frac{dy(\tau)}{d\tau} = 2\sqrt{y}\,\{y_f - y(\tau)\} \tag{C.7}$$

where we introduced the dimensionless final temperature $y_f = T_f/T_0$ defined (as in the main text) by

$$y_f = 1 + \frac{x^2(0)}{3} \tag{C.8}$$

Equation (C.7) can then be rewritten as

$$\int_1^{y(\tau)} \frac{dv}{\sqrt{v}\,(y_f - v)} = 2\tau \tag{C.9}$$

The left-hand-side of (C.9) can be integrated using the result

$$\int \frac{dv}{\sqrt{v}\,(1-v)} = -2\log\left[\tan\left(\frac{\arccos\sqrt{v}}{2}\right)\right] + C \tag{C.10}$$

where C is an integration constant. $y(\tau)$ is thus obtained as the implicit solution of

$$\log\left[\frac{\tan[(\arccos\{[y(\tau)/y_f]^{1/2}\})/2]}{\tan[\{\arccos[(1/y_f)^{1/2}]\}/2]}\right] = 2\sqrt{y_f}\,\tau \tag{C.11}$$

Inversion of (C.11) leads, after a straightforward calculation and returning to the original variables (t, v, T), to the final result (32) for the time dependence of the temperature. On the other hand, the relation (33) between the fluid velocity $v(t)$ and the temperature $T(t)$ can be derived directly from Eqs. (C.6) and (C.1).

ACKNOWLEDGMENTS

L.B. is very grateful to Jean-Louis Barrat for many fruitful discussions. The authors thank H. van Beijeren for attracting their attention to the work of Alley and Alder. J.P. gratefully acknowledges the support of the Centre National de la Recherche Scientifique and of the Conseil Régional Rhône-Alpes during his stay at Laboratoire de Physique de l'École Normale Supérieure de Lyon, where most of this work was carried out.

REFERENCES

1. L. D. Landau and E. M. Lifshitz, *Fluid Mechanics* (Pergamon Press, London, 1963).
2. J. Kirkwood, *J. Chem. Phys.* **14**:180 (1946).
3. P. Español and J. Zúñiga, *J. Chem. Phys.* **98**:574 (1993).
4. J. R. Dorfman and H. van Beijeren, in *Statistical Mechanics*, Part B, B. J. Berne, ed. (Plenum Press, New York, 1977).
5. M. P. Allen and D. J. Tildesley, *Computer Simulations of Liquids* (Clarendon Press, Oxford, 1987).
6. L. Bocquet, J. Piasecki, and J. P. Hansen, *J. Stat. Phys.* **76**:505 (1994).
7. W. Sung and G. Stell, *J. Chem. Phys.* **77**:4636 (1982).
8. R. I. Cukier and J. M. Deutch, *Phys. Rev.* **177**:240 (1969).
9. W. E. Alley, Ph.D. Thesis, Lawrence Livermore Laboratory report UCRL-52815 (1979); B. J. Alder and W. E. Alley, in *Molecular Structure and Dynamics*, M. Balaban, ed. (International Science Services, 1980).
10. T. E. Wainwright, *J. Chem. Phys.* **40**:2932 (1964).
11. G. Ciccotti and W. G. Hoover, eds., *Molecular Dynamics Simulations of Statistical-Mechanical Systems* (North-Holland, Amsterdam, 1986).
12. W. G. Hoover, *Computational Statistical Mechanics* (Elsevier, Amsterdam, 1991).
13. H. Reiss, H. L. Frisch, and J. L. Lebowitz, *J. Chem. Phys.* **31**:369 (1959).
14. B. J. Alder, D. M. Gass, and T. E. Wainwright, *J. Chem. Phys.* **53**:3813 (1970).
15. L. Bocquet and J.-L. Barrat, *Phys. Rev. Lett.* **70**:2726 (1993).
16. J. P. Hansen and I. R. McDonald, *Theory of Simple Liquids*, 2nd ed. (Academic Press, London, 1986).
17. E. H. Hauge and A. Martin-Löf, *J. Stat. Phys.* 7:259 (1973).